Effect of Low-Temperature Plasma Jet on Thermal Stability and Physical Structure of Type I Collagen

Valérie Samouillan, Nofel Merbahi, Mohammed Yousfi, Jean-Pierre Gardou, Florian Delaunay, Jany Dandurand, Colette Lacabanne

Effect of Low-Temperature Plasma Jet on Thermal Stability and Physical Structure of Type I Collagen

Valérie Samouillan, Nofel Merbahi, Mohammed Yousfi, Jean-Pierre Gardou, Florian Delaunay, Jany Dandurand, and Colette Lacabanne

***Abstract*—This work is devoted to the characterization of type I collagen treated by a low-temperature plasma jet generated in ambient air to determine whether the resulting fibrous material is structurally preserved or reinforced. The physical structure of collagen is checked by differential scanning calorimetry (DSC), which is a well suited technique to analyze thermal transitions in proteins, such as denaturation. DSC is used to evaluate the thermal stability of collagen after the plasma treatments while Fourier transform infra red spectroscopy is used to check the integrity of triple helical domain and to investigate the effects of plasma treatments on the functional groups of collagen. It is more particularly shown that the plasma treatment can stabilize the collagen structure without altering the triple helical structure. This observation is supported by 1) the shift observed toward high-temperature range of the collagen denaturation and 2) the stiffening of the chains by a cross-linking action when compared to the control sample.**

***Index Terms*—Denaturation, differential scanning calorimetry (DSC), Fourier transform infra red (FTIR) spectroscopy, low-temperature plasma jet, type I collagen.**

I. Introduction

DEVELOPMENT of biomaterials used as substitutes of the extracellular matrix for the replacement of cardiovascular tissues in associated pathologies or the realization of skin substitutes is a great challenge of repair medicine. Since two decades, detergent and enzymatic protocols have been optimized to obtain non antigenic extracellular matrices, preserving the main fibrillar proteins such as collagen and elastin [1]–[3]. The most commonly utilized collagen, collagen type I, is constituted by triple helices units stabilized by covalent intermolecular cross-links [4]–[8]. The rich chemistry of collagen allows engineers to alter physicochemical properties such as porosity, crystallinity, and cross-link density, resulting in predictable tissue ingrowth and biodegradable rates [9]. Nevertheless, the durability of collagen-based bioprostheses must be improved by the mechanical stabilization of proteins, and their preserving against proteolytic degradation is necessary to a complete recellularization [10].

One of the best methods to preserve collagen is the cross-linking of collagenic fibers in order to restitute the tridimensional network of the protein generally impaired by the cellular purification of tissues [11], [12]. This cross-linking can be achieved by chemical methods (glutaraldehyde, widely used in surgery or carboimides) or by physical methods, such as dehydrothermal treatment or gamma rays or UV irradiation. The main disadvantage of chemical treatment using aldehydes for collagen cross-linking is the cytotoxicity and the calcification of fibers, decreasing the durability of the bioprosthesis [10], [13]. The physical treatments could have the advantage to lead the formation of chemical bonds between collagen macromolecules without the incorporation of any exogenous molecules. For instance, UV treatments have been investigated to cross-link collagen [14], although irradiation can cause both stabilization and destabilization of the collagen structure [14]–[16]. Under such a context, it seems interesting to investigate the effects of nonthermal atmospheric pressure plasmas as they are not yet used for the treatment of collagen fibers, but already successfully used in various other biomedical applications. This concerns plasma sterilization and decontamination of surfaces [17], [18], tissues engineering and biomaterial treatment for their functionalization [19], [20] and more recently plasma medicine for blood coagulation, disinfection of living tissues involving wound healing, and more generally the interaction of plasmas with eukaryotic cells [21]–[24].

Therefore, the aim of this work is to analyze some effects of atmospheric pressure nonthermal plasmas on collagen fibers. We used more particularly a low-temperature plasma jet generated in ambient air [25] and producing various active species (excited species, free radicals, charged particles, and photons (covering a large spectrum from UV up to visible) that are in contact with type I collagen fibers under both freeze-dried and hydrated states.

To quantify the effect of the plasma treatment on the properties of type I collagen, we chose to combine two suitable protein characterization methods: differential scanning calorimetry (DSC) and Fourier transform infra red (FTIR) spectroscopy. DSC is a powerful technique providing direct measurements of thermodynamic characteristics and, unlike the other methods, is efficiently applicable to collagen solutions, fibers, and tissues. It is widely used in collagen research to infer the level of cross-linking within a given sample through elucidation of its denaturation temperature. Furthermore, FTIR spectroscopy is

V. Samouillan, F. Delaunay, J. Dandurand, and C. Lacabanne are with the Université de Toulouse, CIRIMAT-Institut Carnot-UMR 5085, 31062 Toulouse Cedex 9, France (e-mail: valerie.samouillan@iut-tlse3.fr; florian.delaunay@gmail.com; danduran@cict.fr; lacabane@cict.fr).

N. Merbahi and J.-P. Gardou are with the Université de Toulouse, LAPLACE, UMR CNRS 5213, 31062 Toulouse Cedex 9, France (e-mail: nofel.merbahi@Laplace.univ-tlse.fr; gardou@Laplace.univ-tlse.fr).

M. Yousfi is with the Université de Toulouse, LAPLACE, UMR CNRS 5213, Université Paul Sabatier, 31062 Toulouse Cedex 9, France (e-mail: yousfi@Laplace.univ-tlse.fr).

Digital Object Identifier 10.1109/TPS.2012.2190303

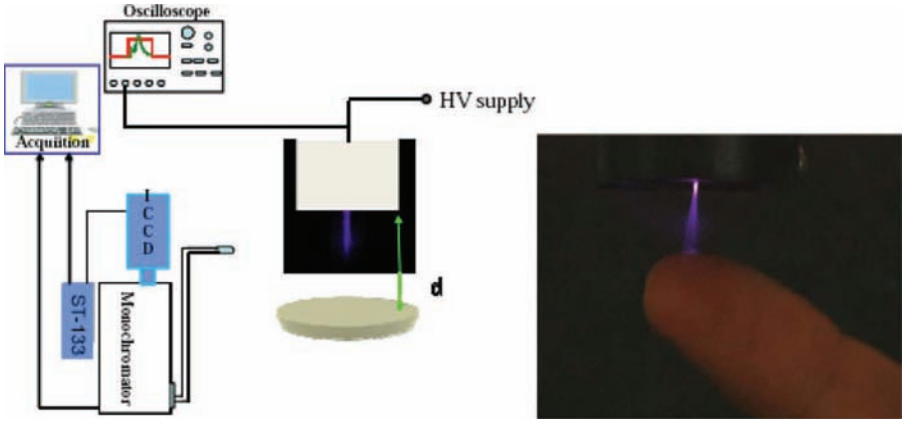

Fig. 1. Overview on the right side on the experimental setup up for plasma jet in ambient air with the spectroscopic coupled ICCD camera and electric (oscilloscope) tools for measurements NB. (a) The treated collagen is schematically displayed at distance d from the plasma jet). (b) The left side picture shows a finger exposed to the low-temperature plasma jet (the temperature of the top of the jet does not exceed 27 °C).

a useful method to monitor changes in secondary structures of a protein, in particular variation in the amide A, amide B, amide I, II, and III regions.

II. Experimental Setups and Method of Analysis

A. Overview on Low-Temperature Plasma Jet

There are in the literature many devices developed to produce a low-temperature plasma jet more particularly for biomedical applications as emphasized in the review of Laroussi [26]. A plasma jet allows a remote treatment very practical for in vivo treatment where it is dangerous to put the living tissue inside the zone of plasma generation. A plasma jet is also very interesting for biomaterial treatment more particularly when it is needed for instance to immerse the biomaterial in water for a treatment under hydrated mode. There are many examples of plasma jet devices for instance plasma needle [27], plasma pencil [28], plasma brush [29], and other setups of plasma jets driven by various power supplies (dc, ac, or RF sources). Such plasma devices generally produce low-temperature plasmas using various gas compositions and designs of the electrode configuration. This allows the launching of the plasma outside the generation zone with the help of a continuous gas flow. The low-temperature plasma jet used in the present work for the collagen treatment has been the subject of a patent [25]. The measured plasma temperature on the top of the jet, that has a length of about 1 cm, does not exceed 27 °C. The plasma jet is generated directly in the ambient air at atmospheric pressure and launched by itself without any system of gas inlet feed. This means that it is easily transportable because there is neither gas bottle nor gas pumping. It is a low-temperature plasma generated by a specific corona discharge design giving a natural repetitive discharge current with a frequency of about 20 kHz under a high-voltage dc power supply. Fig. 1 shows an overview on the experimental setup involving schematically the plasma jet power supply, the tools of measurements (monochromator for spectroscopy and oscilloscope for electric data). Fig. 1 also displays a schematic view of the plasma jet and the treated collagen placed at a distance d from the plasma. Fig. 2(a) shows the instantaneous discharge current with a peak of about 11 mA that corresponds to a dissipated power of about 100 mW. The UV-visible spectrum corresponding to the light emission of the top of the air plasma jet is shown in Fig. 2(b) and (c). This shows the classical emission bands of nitrogen such as the second positive system of $N_2(C_3\pi_u)_v \rightarrow N_2(B_3\pi_g)'_v$ from about 290 nm up to 440 nm corresponding to the different vibration states v and v' (for instance at the peaks at 315.93 nm, 337.13 nm, 357.69 nm, 375.54 nm, and 380.49 nm). The first positive system $N_2(B^3\prod_g) \rightarrow N_2(A_3\Sigma_u^+)$ which is apparent in the visible-near infrared (between about 600 nm up to 900 nm) range indicates the formation of the metastable $N_2(A^3\Sigma_u^+)$ states. The detection of the first negative system (FNS) of $N_2^+(B_2\Sigma_u^+) \rightarrow N_2^+(X_2\Sigma^+g)$ around 390 nm is synonymous of high electron energies leading to the ion formation. However, the presence of positive nitrogen ion is probably very low due to the very small intensity of the FNS emission. There are also the oxygen emissions at for instance 759 nm coming from the band $O_2(b^1\Sigma_g^+ v=0) \rightarrow O_2(X_3\Sigma_g^-, v=0)$ and the atomic line of the triplet state of O at 777.47 nm. An atomic line of nitrogen for N $^4P - ^4 S^0$ is also observable. However, the NO_γ bands due to the emission of $NO(A^2\Sigma^+)_v \rightarrow NO(X^2\prod)'_v$ synonymous of dissociation of molecular nitrogen and oxygen leading to NO formation, are not observable between about 200 nm up to 290 nm due to the quenching of NO_γ bands by the molecular oxygen following the reaction:

$NO(A^2\Sigma^+) + O_2 \rightarrow NO(X^2\prod) + O_2$ with a rate coefficient that is 1000 times higher than the $NO(A^2\Sigma^+)$ quenching by N_2.

The same remark is true for the $OH(A^2\Sigma^+) \rightarrow OH(X^2\prod_{3/2})$ emission bands between about 300 nm up to 320 nm coming from the dissociation of water vapor impurities present in ambient air and not observed due to the quenching by molecular oxygen following the reaction:

$OH(A^2\Sigma^+) + O_2 \rightarrow OH(X^2\prod_{3/2}) + O_2$ with a rate coefficient that is roughly 10 times higher than the $OH(A^2\Sigma^+)$ quenching by N_2.

This overview on plasma jet spectrum means that the excited species present at the top of jet are at least those involved by the emission bands such as $N2(C_3\pi_u)_v$, $N_2(B_3\pi_g)'_v$, $O_2(b^1\Sigma_g^+ v=0)$, $O_2(X^3\Sigma_g^-, v=0)$, $N_2(A^3\Sigma_u^+)$, O and N. Due to the kinetics

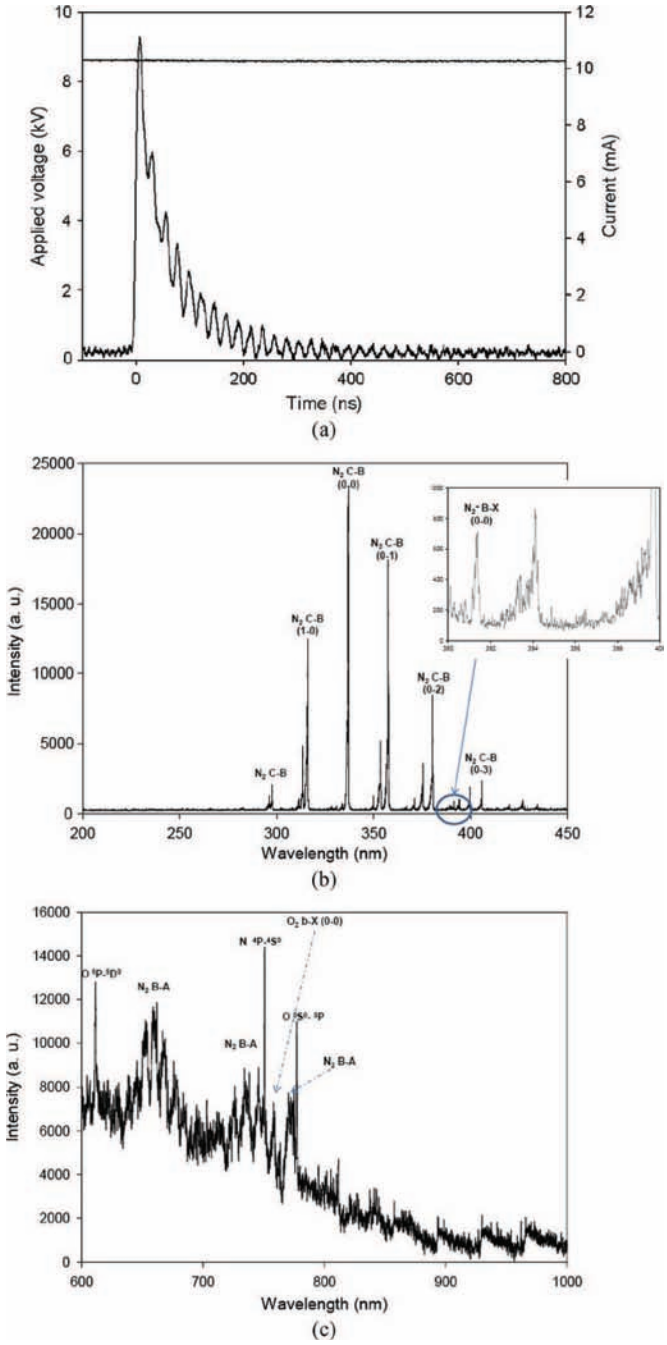

Fig. 2. (a) Instantaneous current of the corona discharge generating the plasma jet in ambient atmospheric pressure air. (b) Spectrum in the 200 nm–450 nm range collected in the top of the plasma jet. (c) Spectrum in the 600 nm–1000 nm range collected in the top of the plasma jet.

of formation of such excited species, it is obvious that we have also another metastable states of molecular nitrogen and oxygen, and also dissociation products of air such as atomic nitrogen N and even atomic hydrogen. There are also other species in the present ambient air plasma jet that are active during the collagen treatment but they are not always detectable in the optical emission spectrum of Fig. 2 due to mainly the quenching processes or to emission outside the present wavelength range (for instance specific atomic lines of nitrogen are in the VUV range below 200 nm).

B. Treated Collagens

Commercial insoluble type I collagen (Fluka Chemie AG, Switzerland) was extracted from bovine Achilles tendon and available in the form of air-dried fibers. The type I collagen is considered under two states:

- *Freeze-dried state*: Collagen fibers were compressed into pellets (thickness 0.5 mm, diameter 10 mm), and each face of the pellet was exposed to the plasma jet during 5, 10, and 60 min at ambient temperature (20 °C). These times were found after preliminary tests to be representative of short and long exposure times.
- *Hydrated state*: 80 mg of collagen fibers was placed in 7 mL of deionized water, equilibrated for 1 h so that the fibers are swollen and subsequently exposed to the plasma jet during 10, 20, 45, and 90 min under stirring at ambient temperature (20 °C). As in the dehydrated state, these times were found to be representative of short and long exposure times.

A set of samples were then carefully put on absorbent paper to remove excess water before thermal analysis. Another set of samples were freeze-dried again before further thermal analysis.

C. Setups of DSC and FTIR Spectroscopy

The DSC phase transition thermograms were recorded with a Pyris Diamond differential scanning calorimeter from Perkin Elmer. The temperature and energy scales were calibrated using the manufacturer's instructions with mercury, indium, and tin as standards. Samples of 5 mg of weight were sealed in aluminum pans. Empty pans were used as references. Thermal analysis is performed to get insight into the denaturation phenomenon of collagen, occurring in the [40 °C; 80 °C] temperature range in the hydrated state and in the [180 °C; 230 °C] in the dehydrated state [8]. That is why investigations in the hydrated state were performed between 10 °C and 90 °C with 10 °C/min heating rates, in hermetic pans. Investigations of the dehydrated state were performed between 30 °C and 250 °C with 10 °C/min heating rates, in nonhermetic pans. Determination of transition parameters was performed with Origin software.

The FTIR spectra were performed in the attenuated total reflection infrared spectroscopy using a Nicolet 5700 FTIR (Thermo Electron Corporation) equipped in ATR device with diamond crystal. All spectra were recorded in absorption mode between 4000 cm^{-1} and 450 cm^{-1} at 4 cm^{-1} interval and 64 accumulations. Spectra were performed in duplicate on two series of treated samples to check the reproducibility in the position of absorption bands (inferior to a deviation of 1 cm^{-1}). The background spectrum was subtracted and a baseline correction was performed. Fourier-self-deconvolution (FSD) of the infrared spectra that allows resolution of several overlapping bands [30] was performed in the amid I–II regions to find the position of the different bands using Omnic software.

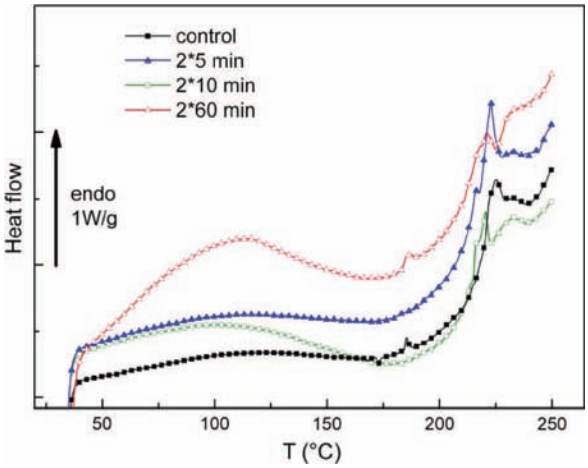

Fig. 3. DSC first scans (from 30 °C to 150 °C, 20 °C/min) of freeze-dried collagens (control and plasma jet-treated collagens).

III. Results and Discussion

The freeze-dried and hydrated collagens are treated by the low-temperature plasma jet for increasing exposures times. The main electric operating parameter of the plasma setup (magnitude of dc voltage of the power supply) is varied within a voltage range between about 8 kV up to 13 kV that allows maintaining the corona regime generating our low-temperature plasma jet. Under these conditions, no change has been observed in the DSC thermograms of the treated collagen. Such results was expected because in this voltage range, only the length of plasma jet undergoes a small variation (10%), but the plasma remains at the same low temperature (because the spark regime, which can heat the plasma, appears only at higher voltages).

A. Freeze-Dried Collagen Treated by Plasma Jet

Fig. 3 shows the DSC thermograms of control collagen and collagen treated by the plasma jet for several time exposures. Table I displays the corresponding denaturation temperatures Td, defined as the maximum of the peak and the corresponding enthalpies of denaturation ΔHd computed from a series of measurements. Calorimetric measurements of control collagen show a broad endothermic phenomenon occurring between 50 °C and 150 °C due to the evaporation and vaporization of residual bound water in collagen [31]. Another endothermic event is observed above 200 °C attributed to the denaturation of collagen. It is addressed to the rupture of hydrogen bonds that maintain the secondary and tertiary structure of collagen inducing the uncoiling of the triple helix in α chains of random conformation, individually or covalently linked depending on the degree of heating [32], [33]. The denaturation of the dry protein occurs in the [180 °C; 250 °C] temperature range as an endothermic peak [34], [35]. The denaturation parameters of the collagen control ($Td = 225$ °C and $\Delta Hd = 7.05$ J $\cdot$ g^{-1}) are similar to thermal parameters of pure freeze-dried collagen generally observed in literature [36]. In this case, the value of the denaturation enthalpy of collagen for hydration $< 6\%$ (corresponding to less than one mole of water per tripeptide) is assigned mainly to the breaking of the direct hydrogen bonds between alpha chains [36].

TABLE I
Denaturation Parameters of Freeze Dried Collagens (Control and Plasma Jet Treated)

Exposure time	ΔHd (J·g^{-1})	Td (°C)
0min(Control)	7.05	225
5 min	13.7	215 - 223
10 min	8.42	215 - 220 - 230
60 min	3.7	217 - 220 - 231

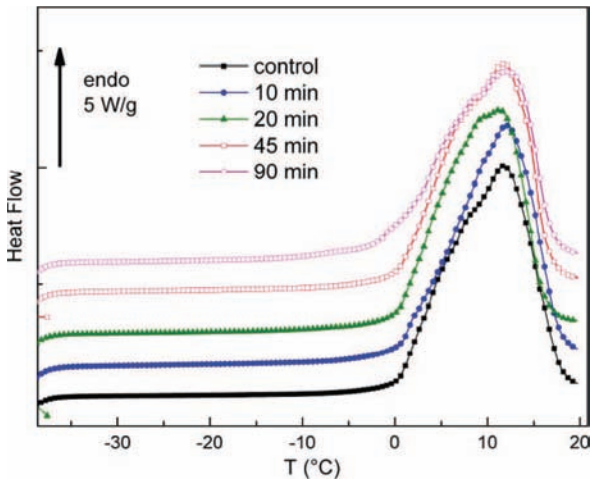

Fig. 4. DSC second scans (from −40 °C to 20 °C, 10 °C/min) of hydrated collagens (control and plasma jet-treated collagens).

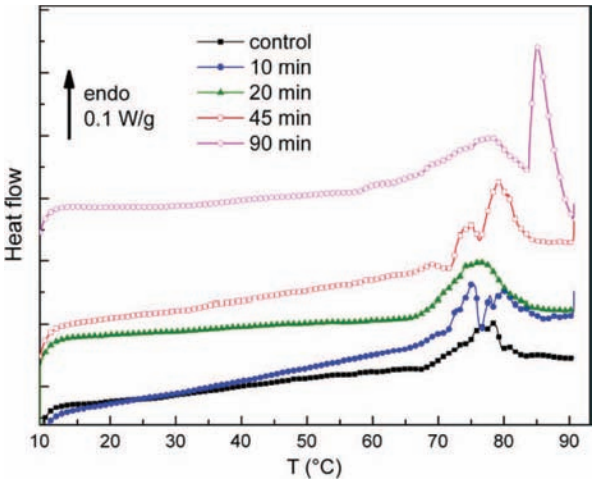

Fig. 5. DSC first scans (from 10 °C to 90 °C, 10 °C/min) of hydrated collagens (control and plasma jet-treated collagens).

In the case of treated collagen, the DSC thermograms (Fig. 3) show several changes. The denaturation becomes a complex event, implying denaturing zones at lower and higher temperature when compared to the control collagen (Fig. 3 and Table I). The destabilized zones could be attributed to the reduction of collagen into polypeptides of different molecular weight [14].

Nevertheless, the high enthalpy associated with destabilized zones for a 5-min exposure is a feature of a triple helical domain. The stabilized zones can be attributed to a cross-linking of collagen. For a 10-min exposure, the total enthalpy is

TABLE II
QUANTIFICATION OF FREE WATER AND TOTAL WATER IN HYDRATED COLLAGENS (CONTROL AND PLASMA JET TREATED)

Exposure time	Ice melting ($J \cdot g^{-1}$)	free water (g/g sample)	Total water (g/g sample)	Hydration (g water/g dry collagen)
0min(Control)	291	0.882	0.917	11.1
10 min	282	0.855	0.898	8.8
20 min	275	0.833	0.883	7.6
45 min	284	0.861	0.902	9.2
90 min	266	0.806	0.864	6.4

slightly greater than the enthalpy corresponding to the control collagen, meaning that the stabilization is mainly entropic, such as induced by an increase in the packing density of collagen molecules in the fibers [17]. For a 60-min exposure time, the shape of denaturation peaks and the low value of the associated enthalpy suggest an important degradation of collagen triple helical structure. The optimum time seems to be comprised between 10 min and 60 min. By increasing exposure time to the low-temperature plasma jet, peptide bond cleavage becomes predominant. The relative proportion of these two competing reactions (cross-linking and bond cleavage) is unknown but was shown to depend on the water content and the oxygen tension [14]. That is why similar experiments were also performed on hydrated collagen.

B. Hydrated Collagen Treated by Plasma Jet

Figs. 4 and 5 display the DSC thermograms (first and second scans) of control collagen (i.e., without plasma treatment) and collagen treated by the plasma jet for gradual exposure times (up to 90 min). The second scan, performed between -40 °C and 20 °C, was used to evaluate free water quantity in collagens. This experiment, that will be discussed in first, was posterior to the analysis of the denaturation zone in order to minimize the influence of calorimetric measures (here a cooling to -40 °C) on the shape of denaturation.

Fig. 4 shows the large endotherm between 0 °C and 20 °C of ice melting. In hydrated collagen, freezable water can be quantified by dividing the area of the measured endotherm by 330 $J \cdot g^{-1}$ corresponding to the melting enthalpy of pure ice. The total amount of water in the collagen sample was evaluated by gravimetry. The quantification of freezable and total water is computed on Table II. Since denaturation parameters are very sensitive to the level of hydration of collagen fibers, we had to check that all the collagens have been analyzed under similar conditions. Some authors [36] showed that the denaturation enthalpy of collagen was constant below 6 moles of water per tripeptide of collagen (corresponding to 0.4 g of water/g collagen), and that the denaturation enthalpy was constant above 30 moles of water per tripeptide (corresponding to 1.9 g of water per g of collagen). Since the levels of hydration in the present study are largely superior to this last limit, we can compare the denaturation parameters versus the exposure time without hydration influence.

In Fig. 5, a complex endothermic peak addressed to the denaturation phenomenon of hydrated collagen is detected for all samples, splitting into two components or more for 10 min, 45 min, and 90 min of plasma exposure. Table III displays the corresponding denaturation temperatures Td and the corresponding denaturation enthalpies ΔHd computed from a series of measurements.

TABLE III
DENATURATION PARAMETERS OF HYDRATED COLLAGENS (CONTROL AND PLASMA JET TREATED)

Exposure time	ΔHd ($J \cdot g^{-1}$ dry collagen)	Td (°C)
0min(Control)	47.8	78.3
10 min	66.4	75.1 – 79.9
20 min	48.8	76.5
45 min	70.6	75.2 -79.1
90 min	126.2	78.0 – 85.1

The denaturation parameters of control hydrated collagen ($Td = 78.3$ °C and $\Delta Hd = 47.8$ J $\cdot$ g^{-1}) are close to thermal parameters of pure freeze-dried collagen generally observed in the literature [36]. The high enthalpy of unfolding collagen immersed in water-when compared with the values found in the dehydrated state-is thought to derive mainly from the breaking of hydrogen bonds forming the hydration network around the collagen molecules. These hydrogen bonds comprise intrachain and interchain as in the dehydrated state but also intermolecular water bridges. More precisely, hydroxyproline and hydroxyl groups are exposed to the solvent and can support hydrogen-bonds water bridges [14], [36], [37].

For 10 min of exposure time, the split of the denaturation peak can be attributed to destabilized zones and stabilized ones, showing in this case as in the dehydrated one the competition between two antagonist processes: reduction into polypeptides of various molecular weights and cross-linking of collagen. The value of enthalpy indicates a conservation of the triple helical structure. Nevertheless, a qualitative comparison between the two peaks shows that the destabilization mechanism is dominant.

For 20 min of exposure time, stabilized zones and destabilized zones must be roughly formed in equal parts, giving rise to a broad and complex denaturation peak.

For 45 min of exposure time, the cross-linking mechanism appears to be the main phenomenon according to peak height and area.

Finally, a special feature is noticed for 90 min of exposure time. Contrary to the evolution at long exposure time reported in the dehydrated case, a sharp and intense peak is detected at 231 °C, corresponding to a highly stabilized collagen domain. The peak previously attributed to destabilized zones is also shifted toward higher temperature, the temperature of the peak maximum being analogous to the control collagen one. Thereofore, the cross-linking mechanism is rather distinct from that observed in the dehydrated state, and seems better to obtain highly stabilized samples.

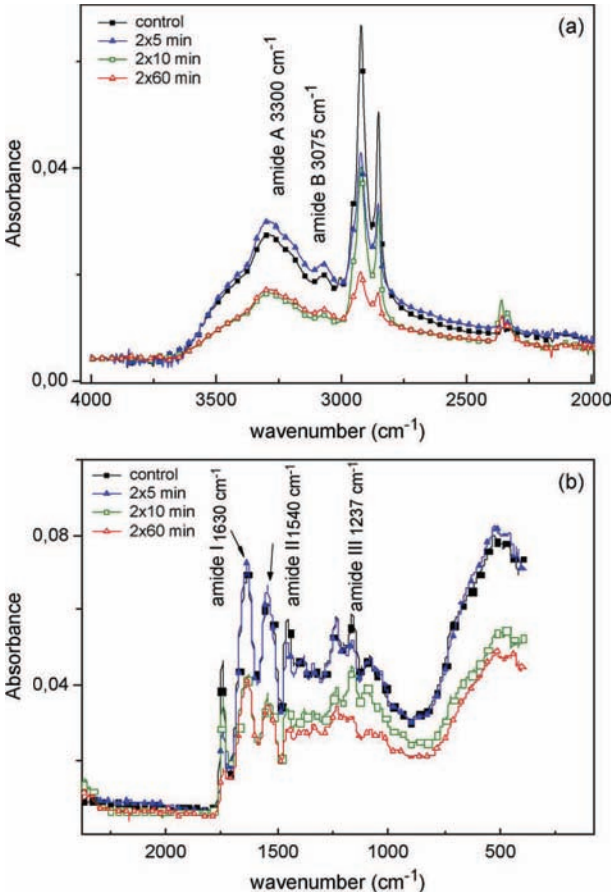

Fig. 6. (a) FTIR spectra of control and plasma-treated collagens in the wavenumber range 4000–2000 cm^{-1}. (b) FTIR spectra of control and plasma-treated collagen in the wavenumber range lower than about 2500 cm^{-1}.

C. FTIR Spectroscopy Analysis of the Treated Freeze-Dried Collagen

The FTIR spectra of protein molecules can be correlated directly to their backbone conformation. The identification of the different absorption bands of the control sample was performed using bibliographic data on collagen type I [38]–[40] and general data on protein FTIR absorption bands [41].

Fig. 6(a) and (b) show the FTIR spectra of the freeze-dried collagen samples decomposed in two wavenumber ranges for a better clarity (4000 cm^{-1} to 2000 cm^{-1} and 2500 cm^{-1} to 400 cm^{-1}). The amide A and B bands at 3300 cm^{-1} and 3075 cm^{-1} [Fig. 6(a)] are mainly associated with the stretching vibrations of N-H groups. The amide I band at 1630 cm^{-1} [Fig. 6(b)] is dominantly attributed to the stretching vibrations of peptide C = O groups. The amide II absorbance at 1540 cm^{-1} [Fig. 6(b)] arises from the N-H bending vibrations coupled to C-N stretching vibrations. The amide III centered at 1237 cm^{-1} [Fig. 6(b)] is assigned to the C-N stretching and N-H bending vibrations from amide linkages, as well as wagging vibrations of CH_2 groups in the glycine backbone and proline side chains [42]. In addition to the amide bands largely exploited for the characterization of proteins, the 3000–2800 cm^{-1} region [Fig. 6(a)] addressed to symmetric and asymmetric stretching modes of CH, CH_2 and CH_3 shows important absorptions due to the high level of aliphatic side chains in collagen.

TABLE IV
IR ABSORPTION RATIO OF AMIDE III (A_{III}) AND 1454 cm-1 WAVENUMBER (A_{1454}) IN THE CASE OF COLLAGEN TREATED BY PLASMA FOR SEVERAL EXPOSURE TIMES AND COMPARED TO CONTROL COLLAGEN (0 min).

Exposure time	A_{III}/A_{1454}
0min (Control)	1.02
5 min	1.02
10 min	1.17
20 min	1.17
60 min	1.16

The superimposition of the spectra of collagen control and plasma-treated collagen indicates that the global positions of the major amide bands do not change with the plasma treatment, particularly the amide I band related to collagen triple helix [43]. Moreover, the IR absorption ratio of amide III to 1454 cm^{-1} (AIII/A1454 cm^{-1}) is also considered to be a measure of the preservation of integrity of collagen triple helices [38], [44] when it is equal or higher than one; it falls to 0.6 for denatured collagen [45]. Table IV shows that the ratios for plasma-treated collagens slightly increase from 1 for control collagen, indicating that the triple helix conformation is not destroyed by the plasma treatment.

Since the amide I–II region consists of several bands strongly dependent on secondary conformations, it was subjected to a FSD in order to resolve the various underlying and overlapping spectral features that contribute to this complex region. The renormalized amide I–II regions and the corresponding FSD traces of control collagen and 60-min treated collagen are presented in Figs. 7(a) and (b).

The amide I region of control collagen results into five components that are the signatures of the different conformations of the protein at 1693 cm^{-1} (antiparallel β-sheets), 1679 cm^{-1} (β-turns), 1660 cm^{-1} (native triple helical conformation), 1645 cm^{-1} (random coil), and 1632 cm^{-1} (β-sheets) [39], [46]–[48]. For 60 min of plasma exposure, the FSD trace confirms the integrity of triple helical conformation (1660 cm^{-1}), and none increase of the random coil conformation (1645 cm^{-1}) as observed in denatured collagen [39]. The main difference concerns the decrease of the absorption in the 1700 cm^{-1}–1680 cm^{-1} region (that gradually decreases upon the time of treatment, results not shown), suggesting a slight modification of the secondary structure of treated collagen in this case, with a diminution of the associated conformations (antiparallel β-sheets and β-turns). Nevertheless, we must take into account that the side chain C = 0 stretching of acid residues (like aspartic acid and glutamic acid, as well as the side chain C = N stretching of basic residue arginine) absorb in the 1700 cm^{-1}–1680 cm^{-1} region, and their contribution is not negligible since their proportion is high in collagen. Also, another possible hypothesis for the diminution of the absorbance in this zone is the modification of these three kinds of residues upon plasma treatment.

Another slight modification concerns the diminution and disappearance of the small absorption band at 3004 cm^{-1}, addressed to the stretching of aromatic and vinylic C-H bonds.

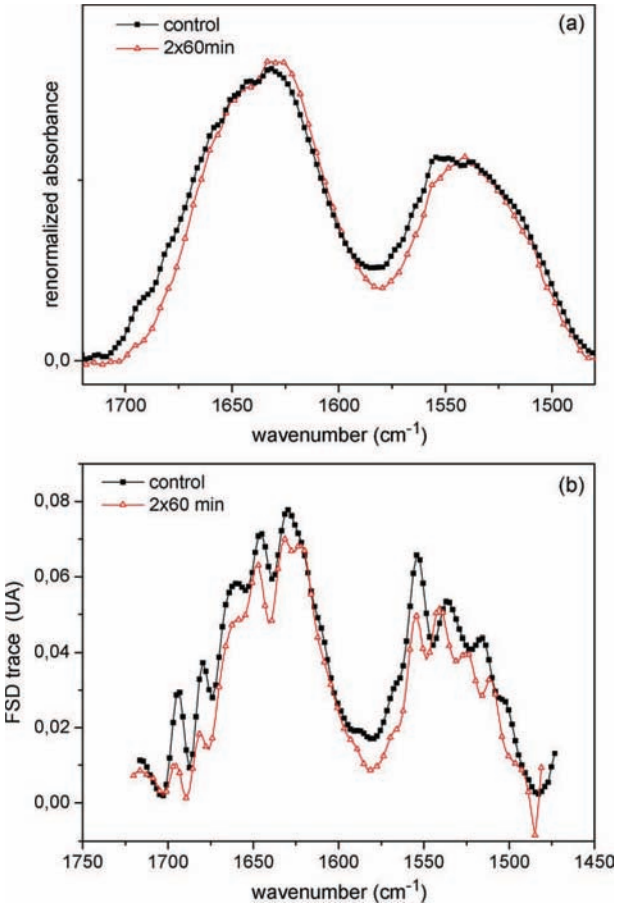

Fig. 7. (a) Renormalized absorbance for amide I–II regions versus wavenumber in the case of control and treated collagen during 2×60 min (60 mn for each side). (b) Fourier-self-deconvolution (FSD) traces for amide I–II regions versus wavenumber in the case of control and treated collagen during 2×60 min (60 min for each side).

Plasma treatment could have an effect of the C = C bond of collagen residues such as tyrosine and phenylalanine. This assertion is corroborated by the modification of the amide II in the 1520–1505 cm^{-1} region, corresponding to the ring mode of tyrosine and phenylalanine. It must be recalled that tyrosine and phenylalanine are the main absorber of UV light that are shown to decrease with UV radiation due to a possible aggregation of the fibers [49].

As the low-temperature plasma jet generates radicals, exited and ionized species and also UV emissions, cross-linking of collagen in our experiments could be partly attributed to the UV emissions of the plasma jet. However, this affirmation must be considered with care because it has to be confirmed by a plasma jet treatment of the collagen done with and without an UV filter. Such a phenomenon was reported both with UVB [14] and UVC [50] irradiation or with the presence of a photosensitizing agent and laser irradiation in the visible spectra [51].

IV. Conclusion

The present work on the thermal denaturation of freeze-dried and hydrated collagens brings us interesting information on the effects of the low-temperature plasma jet treatment on the triple helical structure and the stability of this protein. There is a competition between reduction of collagen in polypeptides and cross-linking mechanisms. In the case of the freeze-dried state, the destabilization of the triple helical structure is the main event for the longest exposure times. The feature is distinct when collagen I fibers are exposed to the plasma jet in the hydrated state. In this case, the cross-linking phenomenon becomes predominant for the longest exposure times (between 45 min and 90 min). Therefore, it is clear that the plasma jet treatment of freeze-dried fibers must be avoided. In addition, it is shown from FTIR analysis slight modifications in absorption bands synonymous to the preservation of the integrity of the triple helical structure of collagen. This however underlines a possible effect of plasma treatment on aromatic side chain and polar side chain of collagen, and could constitute a first step to elucidate the thermal stability enhancement of triple helical structure with the plasma exposure.

The present exploratory work is a first step to determine the effects of low-temperature plasmas generated in ambient air on the preservation of the collagen structure and the enhancement of triple helical stabilization. However, in the light of the present work, it is clear that further investigations are needed to investigate the effects of specific active species on the collagen using other kinds low-temperature plasmas as for instance rare gas-oxygen or rare gas-nitrogen mixtures. Last, it will be very interesting to study in collaboration with biochemists, the biocompatibility and the cellular adhesion and proliferation of the collagenous biomaterials exposed to low-temperature plasma jets.

Acknowledgment

Authors would like to acknowledge UFR PCA of University Paul Sabatier for their financial support.

References

[1] J. M. Lee, C. A. Pereira, and L. W. K. Kan, "Effect of molecular structure of poly(glycidyl ether) reagents on crosslinking and mechanical properties of bovine pericardial xenograft materials," *J. Biomed. Mater. Res.*, vol. 28, no. 9, pp. 981–992, Sep. 1994.

[2] D. W. Courtman, C. A. Pereira, V. Kashef, D. McComb, L. M. Lee, and G. J. Wilson, "Development of a pericardial acellular matrix biomaterial: biochemical and mechanical effects of cell extraction," *J. Biomed. Mater. Res.*, vol. 28, no. 6, pp. 655–666, Jun. 1994.

[3] E. Pasquino, S. Pascale, M. Andreon, S. Rinaldi, F. Laborde, and M. Galloni, "Bovine pericardium for heart valve bioprostheses:in vitro andin vivo characterization of new chemical treatments," *J. Mater. Sci., Mater. Med.*, vol. 5, no. 12, pp. 850–854, Dec. 1994.

[4] T. F. Linsenmayer and T. F. In, *Cell Biology of Extracellular Matrix*, E. D. Hay, Ed., 2nd ed. New York: Plenum, 1991, p. 4.

[5] G. N. Ramanchandran and C. F. Ramakrishnan, *Biochemistry of Collagen*, G. N. Ramanchandran and A. H. Reddi, Eds. New York: Plenum, 1976, p. 45.

[6] M. E. Nimni and R. D. Harness, *Collagen*, M. E. Nimni, Ed. Boca-Raton, FL: CRC Press, 1988, p. 1.

[7] A. J. Hodge and J. A. Petruska, *Aspects of Protein Structure*, G. N. Ramanchandran, Ed. New York: Academic, 1963, p. 289.

[8] J. F. Bateman, S. R. Lamande, and J. A. M. Ramshaw, *Extracellular Matrix: Molecular Components and Interactions*, W. D. Comper, Ed. Boca-Raton, FL: CRC Press, 1996, p. 22.

[9] D. H. Lew, P. H. T. Liu, and D. P. Orgill, "Optimization of UV cross-linking density for durable and nontoxic collagen GAG dermal substitute," *J. Biomed. Mater. Res. B*, vol. 82, no. 1, pp. 51–56, Jul. 2007.

[10] J. L. Hønge, J. A. Funder, H. Jensen, P. M. Dohmen, W. F. Konertz, and J. M. Hasenkam, "Recellularization of decellularized mitral heart valves in juvenile pigs," *J. Heart Valve Dis.*, vol. 19, no. 5, pp. 584–592, Sep. 2010.

[11] W. M. Neethling, R. Glancy, and A. J. Hodge, "Mitigation of calcification and cytotoxicity of a glutaraldehyde-preserved bovine pericardial matrix: improved biocompatibility after extended implantation in the subcutaneous rat model," *J. Heart Valve Dis.*, vol. 19, no. 6, pp. 778–785, Nov. 2010.

[12] M. Madaghiele, A. Piccinno, M. Saponaro, A. Maffezzoli, and A. Sannino, "Collagen- and gelatine-based films sealing vascular prostheses: evaluation of the degree of crosslinking for optimal blood impermeability," *J. Mater. Sci., Mater. Med.*, vol. 20, no. 10, pp. 1979–1989, Oct. 2009.

[13] T. Bottio, V. Tarzia, C. Dal Lin, E. Buratto, G. Rizzoli, M. Spina, A. Gandaglia, F. Naso, and G. Gerosa, "The changing hydrodynamic performance of the decellularized intact porcine aortic root: considerations on in-vitro testing," *J. Heart Valve Dis.*, vol. 19, no. 4, pp. 485–491, Jul. 2010.

[14] A. Sionkowska, "Thermal stability of UV-irradiated collagen in bovine lens capsules and in bovine cornea," *J. Photochem. Photobiol. B*, vol. 80, no. 2, pp. 87–92, Aug. 2005.

[15] C. M. Dong, X. Wu, J. Caves, S. S. Rele, B. S. Thomas, and E. L. Chaikof, "Photomediated crosslinking of C6-cinnamate derivatized type I collagen," *Biomaterials*, vol. 26, no. 18, pp. 4041–4049, Jun. 2005.

[16] P. Ohan, K. S. Weadock, and M. G. Dunn, "Synergistic effects of glucose and ultraviolet irradiation on the physical properties of collagen," *J. Biomater. Res.*, vol. 60, no. 3, pp. 384–391, Jun. 2002.

[17] J. P. Sarrette, S. Cousty, N. Merbahi, A. Nègre-Salvayre, and F. Clément, "Observation of antibacterial effects obtained at atmospheric and reduced pressures in afterglow conditions," *Eur. Phys. J. Appl. Phys.*, vol. 49, no. 1, p. 13 108, Jan. 2010.

[18] S. Villeger, J. P. Sarrette, and A. Ricard, "Synergy between N and O atom action and substrate surface temperature in a sterilization process using a flowing $N_2 - O_2$ microwave post discharge," *Plasma Processes Polym.*, vol. 2, no. 9, pp. 709–714, Nov. 2005.

[19] E. Sardella, L. Detomaso, R. Gristina, G. Senesi, H. Agheli, D. Sutherland, R. d'Agostino, and R. P. Favia, "Nano-structured cell-adhesive and cell-repulsive plasma-deposited coatings: Chemical and topographical effects on keratinocyte adhesion," *Plasma Process. Polym.*, vol. 5, no. 6, pp. 540–551, Aug. 2008.

[20] T. Desmet, R. Morent, N. De Geyter, C. Leys, E. Schacht, and P. Dubruel, "Nonthermal plasma technology as a versatile strategy for polymeric biomaterials surface modification: a review," *Biomacromolecules*, vol. 10, no. 9, pp. 2351–2378, Sep. 2009.

[21] G. E. Morfill, M. G. Kong, and J. L. Zimmerman, "Nosocomial infections—A new approach towards preventive medicine using plasmas," *New J. Phys.*, vol. 11, p. 115011, Nov. 2009.

[22] E. Stoffels, A. J. M. Roks, and E. Deelman, "Delayed effects of cold atmospheric plasma on vascular cells," *Plasma Process. Polym.*, vol. 5, no. 6, pp. 599–605, Aug. 2008.

[23] G. Lloyd, G. Friedman, S. Jafri, G. Schultz, A. Fridman, and K. Harding, "Gas plasma: Medical uses and developments in wound care," *Plasma Process. Polym.*, vol. 7, no. 3/4, pp. 194–211, Mar. 2010.

[24] D. Dobrynin, G. Fridman, G. Friedman, and A. Fridman, "Physical and biological mechanisms of direct plasma interaction with living tissue," *New J. Phys.*, vol. 111, p. 115020, Nov. 2009.

[25] N. Merbahi, M. Yousfi, and O. Eichwald, "Device for emitting a plasma jet from the atmospheric pressure air at ambient temperature and pressure, and use of said device," International Publication Patent WO 2011/00170 A1, Jun. 1, 2011.

[26] M. Laroussi and T. Akan, "Arc-free atmospheric pressure cold plasma jets: A review," *Plasma Process. Polym.*, vol. 4, no. 9, pp. 777–788, Nov. 2007.

[27] I. E. Kieft, D. Darios, A. J. M. Roks, and A. J. M. E. Stoffels, "Plasma treatment of mammalian vascular cells: a quantitative description," *IEEE Trans. Plasma Sci.*, vol. 33, no. 2, pp. 771–775, Apr. 2005.

[28] M. Laroussi and X. Lu, "Room-temperature atmospheric pressure plasma plume for biomedical applications," *Appl. Phys. Lett.*, vol. 87, no. 11, pp. 113 902-1–113 902-3, Sep. 2005.

[29] Y. Duan, C. Huang, and Q. Yu, "Low-temperature direct current glow discharges at atmospheric pressure," *IEEE Trans. Plasma Sci.*, vol. 33, no. 2, pp. 328–329, Apr. 2005.

[30] X. Hu, D. Kaplan, and P. Cebe, "Determining beta sheet crystallinity in fibrous proteins by thermal analysis and infrared spectroscopy," *Macromolecules*, vol. 39, no. 18, pp. 6161–6170, 2006.

[31] V. Samouillan, J. Dandurand-Lods, A. Lamure, E. Maurel, C. Lacabanne, G. Gerosa, A. Venturini, A. Casarotto, L. Gherardini, and M. Spina, "Thermal analysis characterization of aortic tissues for cardiac valve bioprostheses," *J. Biomed. Mater. Res.*, vol. 46, no. 4, pp. 531–538, Sep. 1999.

[32] P. L. Privalov, E. I. Tiktopulo, and V. M. Tischenko, "Stability and mobility of the collagen structure," *J. Mol. Biol.*, vol. 127, no. 2, pp. 203–216, Jan. 1979.

[33] G. Balian and J. H. Bowes, *In: The Structure and Properties of Collagen*, A. G. Ward and A. Courts, Eds. London, U.K.: Academic, 1977, p. 1.

[34] V. Samouillan, A. Lamure, E. Maurel, J. Dandurand, C. Lacabanne, and M. Spina, "On the molecular basis of fouling resistance," *J. Biomater. Sci. Polym. Ed.*, vol. 11, no. 6, pp. 547–569, 2000.

[35] V. Samouillan, A. Lamure, E. Maurel, J. Dandurand, C. Lacabanne, F. Ballarin, and M. Spina, "Characterisation of elastin and collagen in aortic bioprotheses," *Med. Biol. Eng. Comput.*, vol. 38, no. 2, pp. 226–231, Mar. 2000.

[36] C. Miles and M. Ghelashvili, "Polymer-in-a-box mechanism for the thermal stabilization of collagen molecules in fibers," *Biophys. J.*, vol. 76, no. 6, pp. 3243–3252, Jun. 1999.

[37] C. Miles, A. Sionkowska, S. Hulin, T. J. Sims, N. C. Avery, and A. J. Balley, "Identification of an intermediate state in the helix-coil degradation of collagen by ultraviolet light," *J. Biol. Chem.*, vol. 275, no. 42, pp. 33 014–33 020, Oct. 2000.

[38] L. He, C. Mu, J. Shi, Q. Zhang, B. Shi, and W. Lin, "Modification of collagen with a natural cross-linker, procyanidin," *Int. J. Biol. Macromol.*, vol. 48, no. 2, pp. 354–359, Mar. 2011.

[39] O. S. Rabotyagova, P. Cebe, and D. L. Kaplan, "Collagen structural hierarchy and susceptibility to degradation by ultraviolet radiation," *Mater. Sci. Eng.*, vol. C28, pp. 1420–1429, 2008.

[40] A. Sionkowska, J. Skopinska-Wisniewska, M. Gawron, J. Kozlowska, and A. Planecka, "Chemical and thermal cross-linking of collagen and elastin hydrolysates," *Int. J. Biol. Macromol.*, vol. 47, pp. 570–577, 2010.

[41] A. Barth, "The infrared absorption of amino acid side chains," *Progr. Biophys. Mol. Biol.*, vol. 74, no. 3–5, pp. 141–173, 2000.

[42] B. Madhan, V. Subramanian, J. R. Rao, B. U. Nair, and T. Ramasami, "Stabilization of collagen using plant polyphenol: role of catechin," *Int. J. Biol. Macromol.*, vol. 37, no. 1/2, pp. 47–53, Oct. 2005.

[43] K. J. Payne and A. Veis, "Fourier transform ir spectroscopy of collagen and gelatin solutions: Deconvolution of the amide I band for conformational studies," *Biopolymers*, vol. 27, no. 11, pp. 1749–1760, Nov. 1988.

[44] M. E. Andrews, J. Murali, C. Muralidharan, W. Madhulata, and R. Jayakumara, "Interaction of collagen with corilagin (a hydrolysable tannin)," *Colloid Polym. Sci.*, vol. 281, pp. 766–770, 2003.

[45] M. F. Silvester, Y. Yannas, and M. J. Forbes, "Collagen banded fibril structure and the collagen-platelet reaction," *Thromb. Res.*, vol. 55, no. 1, pp. 135–148, Jul. 1989.

[46] R. S. Walton, D. D. Brand, and J. T. Czernuska, "Influence of telopeptides, fibrils and crosslinking on physicochemical properties of type I collagen films," *J. Mater. Sci., Mater. Med.*, vol. 21, no. 2, pp. 451–461, Feb. 2010.

[47] S. Krimm and J. Bandekar, "Vibrational spectroscopy and conformation of peptides, polypeptides, and proteins," *Adv. Protein Chem.*, vol. 38, pp. 181–364, 1986.

[48] A. M. Tamburro, A. Pepe, B. Bochicchio, D. Quaglino, and I. Pasquali Ronchetti, "Supramolecular amyloid-like assembly of the polypeptide sequence coded by Exon 30 of Human Tropoelastin," *J. Biol. Chem.*, vol. 280, no. 4, pp. 2682–2690, Jan. 2005.

[49] Y. Kato, K. Uchida, and S. Kawakishi, "Aggregation of collagen exposed to UVA in the presence of riboflavin: A plausible role of tyrosine modification," *Photochem. Photobiol.*, vol. 59, no. 3, pp. 343–349, Mar. 1994.

[50] A. B. Caruso and M. D. Dunn, "Functional evaluation of collagen fiber scaffolds for ACL reconstruction: cyclic loading in proteolytic enzyme solutions," *J. Biomed. Mater. Res.*, vol. 69, no. 1, pp. 164–171, Apr. 2004.

[51] B. P. Chan and K. F. So, "Photochemical crosslinking improves the physicochemical properties of collagen scaffolds," *J. Biomed. Mater. Res.*, vol. 75, no. 3, pp. 689–701, Dec. 2005.